

Vortex Charging Effect in a Chiral $p_x \pm ip_y$ -Wave Superconductor

Masashige Matsumoto¹ and Rolf Heeb²

¹Department of Physics, Faculty of Science, Shizuoka University, 836 Oya, Shizuoka 422-8529, Japan

²Theoretische Physik, Eidgenössische Technische Hochschule Hönggerberg, CH-8093 Zürich, Switzerland

(August 19, 2019)

Quasiparticle states around a single vortex in a $p_x \pm ip_y$ -wave superconductor are studied on the basis of the Bogoliubov-de Gennes (BdG) theory, where both charge and current screenings are taken into account. Due to the violation of time reversal symmetry, there are two types of vortices which are distinguished by their winding orientations relative to the angular momentum of the chiral Cooper pair. The BdG solution shows that the charges of the two types of vortices are quite different, reflecting the rotating Cooper pair of the $p_x \pm ip_y$ -wave paring state.

PACS numbers: 74.60.Ec, 74.25.Jb, 74.60.Ge, 71.27.+a

The discovery of many types of superconductors from heavy fermion compounds to high- T_c cuprates has driven us to study a large variety of new physics beyond the standard BCS theory for conventional s -wave superconductors. To understand the nature of the unconventional superconducting states, much effort has been made to specify their order parameters [1]. The study of the unconventional superconductivity was stimulated by the discovery of superfluid ^3He in which a spin triplet p -wave state realizes. Unlike the conventional s -wave state, the p -wave state has both spin and orbital degrees of freedom [2]. This is the most pronounced feature of the unconventional superconductors observed in their thermodynamics and impurity effects or detected by tunneling spectroscopy, NMR, μSR measurements, and so on.

Sr_2RuO_4 is the first layered perovskite compound showing superconductivity without CuO_2 planes [3]. The recent experimental and theoretical studies have indicated that the superconducting pairing symmetry of Sr_2RuO_4 is not a simple s -wave. The absence of a Hebel-Slichter peak in NQR [4] and the sensitivity of T_c on non-magnetic impurities [5] clearly point towards unconventional pairing. Moreover, the indication of broken time reversal symmetry in the superconducting phase [6], observed in μSR measurements, gives a strong argument for the unconventional paring state. The most decisive clue for spin-triplet pairing comes from the Knight shift experiment which shows that the spin susceptibility is not affected by the superconducting state [7]. Anomalous temperature dependence of the critical current of a Josephson junction between Sr_2RuO_4 and Pb also supports the unconventional paring state [8,9]. Sigrist *et al.* suggested that a $p_x \pm ip_y$ -wave state, which breaks the time reversal symmetry in a tetragonal crystal field, is the most likely pairing state for Sr_2RuO_4 [10]. The line node behavior is reported in the latest experiments [11,12] related to the low temperature thermodynamical measurements, such as specific heat and NMR T_1^{-1} . An orbital dependent superconductivity [13] and gap anisotropy [14] were suggested to understand the line node behavior. Here we focus on the $p_x \pm ip_y$ -wave pairing state, since this rep-

resentation is the simplest and essential form. We will see rich physics of this chiral state, which breaks time reversal symmetry.

The most intriguing character of the $p_x \pm ip_y$ -wave state is that the Cooper pair has ± 1 angular momentum, i.e. the pair electrons are rotating. This property is similar to that of the A phase of the superfluid ^3He . Due to the violation of the time reversal symmetry, we have two types of vortices, one of which is in the same direction to the angular momentum of the rotating Cooper pair, and the other is in the opposite direction. Therefore it is important to study an isolated single vortex, since this rotating pair shows up in quasiparticle states around a vortex core.

In this letter we present an interesting new physics related to a vortex. We focus on a vortex charging effect [15]. It was pointed out that for an s -wave superconductor the vortex charge is proportional to the slope of the density of states at the Fermi level [16]. Hayashi *et al.* has proposed that the vortex charge is determined by the detailed electronic structure in the vortex core [17] rather than the slope of the density of states. Very recently, it has been reported that Chern-Simons terms lead to a fractional vortex charge for the $p_x \pm ip_y$ -wave superconductors [18]. Thus the origin of the vortex charge is still controversial. To make this point clearer, we investigate the vortex charging effect in the chiral $p_x \pm ip_y$ -wave state, concentrating our attention on a microscopic origin of the vortex charge. This is demonstrated by solving the BdG equation self-consistently, including both charge and current screenings. We would like to show how the rotating Cooper pair shows up in the vortex charging effect. We perform full self-consistent calculations for the first time to solve the BdG equation in the presence of a vortex.

Let us begin with the following BdG and gap equations for the $p_x \pm ip_y$ -wave state [19–21]:

$$h_0 u_n - \frac{i}{k_F} \sum_{\pm} \left[\Delta_{\pm} \square_{\pm} + \frac{1}{2} (\square_{\pm} \Delta_{\pm}) \right] v_n = E_n u_n,$$

$$\begin{aligned}
-h_0^* v_n - \frac{i}{k_F} \sum_{\pm} \left[\Delta_{\pm} \square_{\pm} + \frac{1}{2} (\square_{\pm} \Delta_{\pm}) \right]^* u_n &= E_n v_n, \\
\Delta_{\pm}(\mathbf{r}) &= -i \frac{g}{2k_F} \sum_{0 \leq E_n \leq E_c} \tanh\left(\frac{E_n}{2T}\right) \\
&\times [v_n^*(\mathbf{r}) \square_{\mp} u_n(\mathbf{r}) - u_n(\mathbf{r}) \square_{\mp} v_n^*(\mathbf{r})], \quad (1)
\end{aligned}$$

where $h_0 = (-i\nabla + e\mathbf{A}/c)^2/2m - eA_0 - \mu$ ($\hbar = 1, e > 0$). E_n is the energy eigen value for the superconducting quasiparticle, and $\square_{\pm} = \partial_x \pm i\partial_y$ is used. In the presence of electromagnetic fields, scalar (A_0) and vector (\mathbf{A}) potentials are introduced. g is a coupling constant for the p -wave paring, E_c is a cutoff energy, and μ is a chemical potential. Δ_{\pm} is the order parameter for the $p_x \pm ip_y$ -wave paring state, which is a real function of \mathbf{r} . For simplicity, we assume that the superconductor is basically two dimensional and has a cylindrical Fermi surface. We note that the BdG solution has the following time reversal relation:

$$\{u_{-E_n}, v_{-E_n}\} = \{v_{E_n}^*, u_{E_n}^*\}. \quad (2)$$

The solution of the BdG equation determines the two dimensional electron and current densities:

$$\begin{aligned}
n_e(\mathbf{r}) &= 2 \sum_{E_n} |u_n(\mathbf{r})|^2 f(E_n), \\
\mathbf{J}(\mathbf{r}) &= -\frac{ie}{m} \sum_{E_n} [u_n^*(\mathbf{r}) \nabla u_n(\mathbf{r}) - u_n(\mathbf{r}) \nabla u_n^*(\mathbf{r})] f(E_n) \\
&\quad - \frac{e^2}{mc} n_e(\mathbf{r}) \mathbf{A}(\mathbf{r}). \quad (3)
\end{aligned}$$

By using the relation (2), both densities are expressed in terms of the u_n amplitude. $f(E_n)$ is the Fermi distribution function and the E_n summation in Eq. (3) runs both negative and positive regions. The scalar and vector potentials obey the Maxwell equations: $\nabla^2 A_0(\mathbf{r}) = -\frac{4\pi e}{d} [n_0 - n_e(\mathbf{r})]$ and $\nabla^2 \mathbf{A}(\mathbf{r}) = -\frac{4\pi}{cd} \mathbf{J}(\mathbf{r})$. We have introduced a layer spacing d to convert the area densities into the volume ones. To satisfy overall charge neutrality we introduce a uniform n_0 as the density of positive background charge. Since all physical quantities are cylindrical, we take the following forms for the current density and vector potential: $\mathbf{J}(\mathbf{r}) = J_{\phi}(r)\hat{\phi}$ and $\mathbf{A}(\mathbf{r}) = A_{\phi}(r)\hat{\phi}$, where r and ϕ are the two-dimensional polar coordinates, and $\hat{\phi}$ is a unit vector in the ϕ direction. For simplicity, we have taken the origin of the coordinate at the vortex center.

In the bulk region $p_x + ip_y$ and $p_x - ip_y$ -wave states are degenerate. In this letter we will choose one of the two degenerate states, the $p_x + ip_y$ -wave state as a dominant component in the bulk. Even in the $p_x + ip_y$ -wave state, the other component ($p_x - ip_y$) is admixed with the bulk ($p_x + ip_y$) state close to the vortex core [22]. Therefore our formulation includes both $p_x \pm ip_y$ components. The $p_x + ip_y$ -wave state also has its own +1 Cooper pair phase winding, since $\square_+ = e^{i\phi}(\partial_r + \frac{i}{r}\partial_{\phi})$ in Eq. (1). It is well

known that a single vortex has a phase winding ± 1 in the real space order parameter. Therefore there are two kind of vortices: the vortex winding direction is parallel (positive vortex) or anti-parallel (negative vortex) relative to the Cooper pair winding. Thus the P (positive)-vortex has two fold windings +2 effectively. However, in the N (negative)-vortex case, the two types of winding directions are opposite and the Cooper pair cancels the vortex winding. Due to the rotational symmetry of the system, angular momentum is a good quantum number. The BdG equation is then classified by the angular momentum. To overcome the $e^{-i\phi}$ factor which comes from the \square_- operator in Eq. (1), the angular momentum of the admixed component must differ 2 from the dominant one. Therefore the combinations of the dominant and admixed components are given by

$$\begin{aligned}
(P) \quad \Delta_+(\mathbf{r}, \phi) &= \Delta_+(\mathbf{r}) e^{i\phi}, \quad \Delta_-(\mathbf{r}, \phi) = \Delta_-(\mathbf{r}) e^{i3\phi}, \\
(N) \quad \Delta_+(\mathbf{r}, \phi) &= \Delta_+(\mathbf{r}) e^{-i\phi}, \quad \Delta_-(\mathbf{r}, \phi) = \Delta_-(\mathbf{r}) e^{i\phi},
\end{aligned}$$

where Δ_+ and Δ_- are the dominant and admixed components, respectively. The two vortex orientations are denoted by P (positive) and N (negative) vortices. Hence in the BdG equation u_n couples with v_n in the following angular momentum spaces [20]:

$$(P) \quad u_n^l \leftrightarrow v_n^{l-2}, \quad (N) \quad u_n^l \leftrightarrow v_n^l, \quad (4)$$

where the superscripts represent the angular momenta of the wave functions u_n and v_n . Actually the cylindrical symmetry is realized by these combinations. The GL calculation showed that the N-vortex turned out to be energetically favored [23]. However, in a real sample we can expect two types ($p_x \pm ip_y$) of domains, so that there are both P and N-vortices in the presence of an external magnetic field. As we will see later, the difference between the two vortices appears in a vortex charging effect. We solve the two dimensional single vortex problem on a disk of radius R with the same procedure in Ref. [20]. In our numerical calculation, we obtain $\Delta_{\pm}(\mathbf{r})$, $A_0(\mathbf{r})$, and $\mathbf{A}(\mathbf{r})$ by solving Eqs. (1), (3) and the Maxwell equations iteratively within a Gygi and Schlüter method [24]. In the self-consistent calculation we fix the total number of electron to the normal state value by adjusting μ .

Let us discuss our BdG self-consistent solutions. The order parameter Δ_- shows the asymptotic behavior $\Delta_- \propto r$ ($\Delta_- \propto r^3$) for the N-vortex (P-vortex) as shown in Fig. 1(a), which reproduces well the GL result [23]. We notice that $|\Delta_-|$ for the N-vortex is larger than the P-vortex one, which implies that the N-vortex gains much condensation energy. A zero energy bound state appears for both P and N-vortices as shown in Fig. 1(b) [25]. These states appear in an $l_u = 1$ ($l_u = 0$) space for the P-vortex (N-vortex). The appearance of the zero energy states is the consequence of the symmetric property of the BdG equation [Eq. (2)]. P_B and N_B in Fig. 1(b) represent bound states in an $l_u = 0$ angular momentum

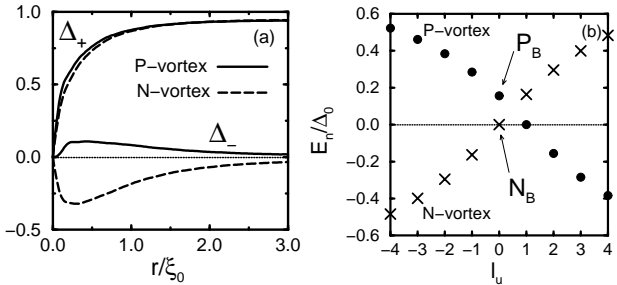


FIG. 1. Self-consistent results at $T = 0$. (a) Order parameters scaled by Δ_0 , which is the magnitude of the order parameter at zero temperature in the bulk region. $\xi_0 = v_F/\Delta_0$ is the coherence length. Set of parameters are taken as $R = 8\xi_0$, $k_F\xi_0 = 16$, $\lambda_L = \xi_0$, $\lambda_{TF} = 1/k_F$, $E_c = \mu$. Here λ_L and λ_{TF} are the London and Thomas Fermi screening lengths, respectively. (b) Bound state energy spectrum for the P-vortex (circle) and N-vortex (X). l_u is the angular momentum of the u wave function. The bound state with $l_u = 0$ P_B (N_B) for the P-vortex (N-vortex) plays an important role in the vortex charging effect (see the text). Extended states lie continuously in a $|E_n| \geq \Delta_0$ region [20].

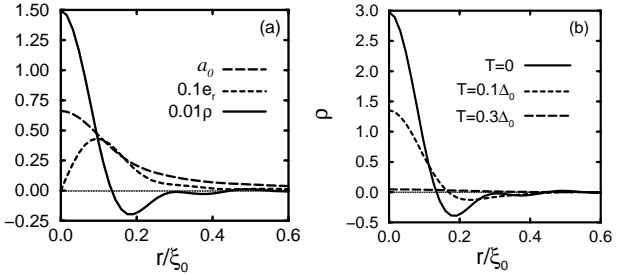


FIG. 2. (a) Dimensionless scalar potential $a_0 = eA_0/\Delta_0$, electric field $e_r = -\xi_0 \partial_r a_0$, and charge density $\rho = \xi_0(1/r + \partial_r)e_r$ for the P-vortex at $T = 0$. (b) Temperature dependence of the P-vortex charge density scaled by e/ξ_0^2 .

space for the P and N-vortices, respectively. We can see in Fig. 2(a) that large charge density appears close to the P-vortex core, while for the N-vortex the charge density is almost zero [26]. In the P-vortex case, the charge density decreases with the increase of temperature [see Fig. 2(b)].

Let us explain the microscopic origin of the vortex charging effect for the chiral $p_x \pm ip_y$ -wave state. First we discuss the P-vortex case. There are two types of electron densities: one is from the bound states (n_B) and the other is from the extended states (n_E) as shown in Figs. 3(a) and (b). We find out the important role of zero angular momentum ($l = 0$) states in this microscopic study [17,26]. In general only $l = 0$ states contribute to the local electron density at the vortex center. At zero temperature only $E_n \leq 0$ states are effective. Therefore the bound state P_B for the P-vortex cannot generate the local electron density at $r = 0$, since the P_B state is not occupied. Hence the total electron density n_T is decreased

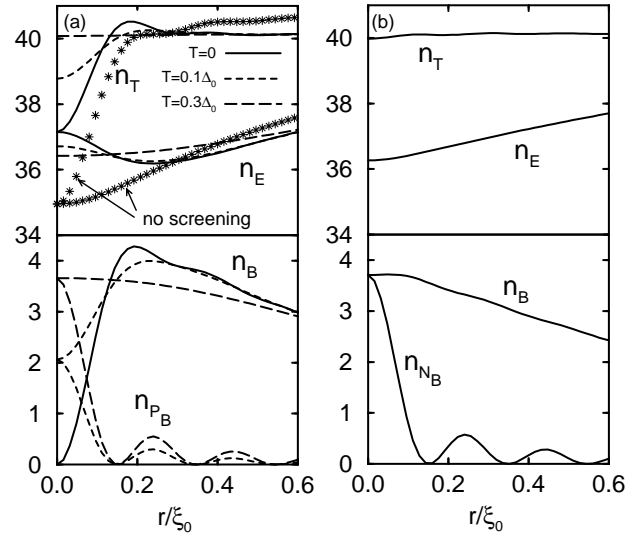


FIG. 3. Local electron density scaled by $1/\xi_0^2$. (a) In the P-vortex case. Subscripts B, E, and T represent the electron densities which come from bound states, extended states, and their total. n_{P_B} is the electron density generated by the $l_u = 0$ bound state P_B presented in Fig. 1(b). n_{P_B} is completely zero at $T = 0$. Lines with stars (*) represent the local electron densities at $T = 0$, where A_0 is neglected (no charge screening). (b) In the N-vortex case at $T = 0$. n_{N_B} is the electron density which comes from the bound state N_B in Fig. 1(b).

near the P-vortex center as shown in Fig. 3(a) due to the lack of the P_B contribution. At finite temperatures the contribution from the P_B state (n_{P_B}) comes out, and it increases n_T at $r = 0$ [see Fig. 3(a)] due to the finite Fermi distribution function in Eq. (3) for the $E_n > 0$ region. At $T = 0.3\Delta_0$, which is larger than the energy of P_B , n_T becomes almost uniform due to the contribution from the P_B state. The vortex charge is then reduced strongly at high temperatures as shown in Fig. 2(b).

Next we discuss the N-vortex case. For the N-vortex n_T is almost uniform as shown in Fig. 3(b). This is because the bound state N_B is located at just zero energy and it can generate the local electron density at $r = 0$. In the N-vortex case the Cooper pair winding cancels the vortex one, so that u_n couples with v_n in an $l = 0$ space in the BdG equation, generating the zero energy N_B state. Since the $l = 0$ quasiparticles do not rotate around the vortex, both u_n and v_n are not affected by a centrifugal force. This explains why the electron density at $r = 0$ is not decreased for the N-vortex. In the N-vortex case we find very small temperature dependence in n_T , since the N_B state has zero energy and participates in the energy excitations with the same rate at any temperature. Notice that the n_B , n_E , and n_T for the N-vortex are similar to those for the P-vortex at $T = 0.3\Delta_0$, where the P_B state is occupied. We conclude that the appearance of the vortex charge depends on the position of the $l_u = 0$ bound state relative to the temperature. In the conven-

tional s -wave case, the vortex charge always appears at sufficiently low temperatures [17], which is similar to the P-vortex result.

Next let us discuss an effect of the charge screening. In Fig. 3(a) we also show the electron densities for the P-vortex where the charge screening is neglected ($A_0 = 0$). We compare the two cases in Fig. 3(a), where the charge is screened or not at $T = 0$. We find enhancement in n_E near $r = 0$ in the charge screening case, whereas the difference in n_B is indistinguishable between the two cases. These results tell us that the extended states screen the vortex charge. Since the bound states are localized around the vortex core, their wave function hardly modulate, while the extended states do easily. Hence the extended states quickly respond to the electric field and they screen the vortex charge.

In general the Chern-Simons physics is related to an interaction between electronic and magnetic fields, so that our result including both A_0 and \mathbf{A} contains the Chern-Simons term. To see an effect of the Chern-Simons term [18], we compare the two results, where \mathbf{A} is present or not (no Chern-Simons term). A_0 is taken into account in both cases. We note that the effect of the Chern-Simons term on the vortex charge is too small to be seen in our numerical results. This implies that the vortex charge is not mainly determined by the Chern-Simons term.

In conclusion, we have solved the problem of a single $p_x \pm ip_y$ -wave vortex self-consistently within the Bogoliubov-de Gennes theory. The full self-consistent calculation including both charge and current screenings was performed for the first time to investigate vortex problems. Due to the time reversal symmetry breaking, there are two types of vortices. We found a substantial vortex charge in the positive vortex case, while the vortex charge is suppressed for the negative vortex. We conclude that the vortex charging effects are mainly determined by the local quasiparticle structure around the vortex core, reflecting the chiral $p_x \pm ip_y$ -wave paring. Especially the lowest vortex bound state is very important for the charging effect.

In a real sample we can expect two types ($p_x \pm ip_y$) of domains. In domains, where the P-vortex is realized, an electronic field is induced due to the large vortex charge. Therefore the charge of the P-vortex can be detected. If we use a field cooled sample, a single domain forming the N-vortex is realized all over the sample, since the N-vortex is energetically favorable [23]. In this case it is difficult to find a signal from the N-vortex, since the charge of the N-vortex is much smaller than the P-vortex one. Thus we can distinguish the two types of P and N-vortices.

How can we detect the vortex charge? The vortex charge can induce lattice distortion and the lattice distortion scatters neutrons. It is reported that a polarized neutron scattering can be used to detect the vortex charge [27]. NQR is also one of the possible experiment

which can detect the vortex charging effect, since the NQR detects the local electric field induced by the vortex charge. Very recently, Kumagai *et al.* reported that the vortex charge is observed by the NQR in a high- T_c material [28]. Thus the detection of the vortex charge is in progress now. It is very exciting if the vortex charge of the chiral superconductor is detected, since it can provide a very strong evidence of the *rotating* Cooper pair.

The authors express their sincere thanks to M. Sigrist and G. Blatter for many stimulating discussions. One of the authors (M. M.) thanks N. Hayashi for helpful discussions. He would like to acknowledge M. Koga for his critical reading of the manuscript. This work is supported by Casio Science Promotion Foundation.

-
- [1] M. Sigrist and K. Ueda, Rev. Mod. Phys. **63**, 239 (1991).
 - [2] D. Vollhardt and P. Wölfle, *The Superfluid Phases of Helium 3* (Taylor and Francis, London, 1990).
 - [3] Y. Maeno *et al.*, Nature **372**, 532 (1994).
 - [4] K. Ishida *et al.*, Phys. Rev. B **56**, R505 (1997).
 - [5] A. P. Mackenzie *et al.*, Phys. Rev. Lett. **80**, 161 (1998).
 - [6] G. M. Luke *et al.*, Nature **394**, 558 (1998).
 - [7] K. Ishida *et al.*, Nature **396**, 658 (1998).
 - [8] R. Jin *et al.*, Phys. Rev. B **59**, 4433 (1999).
 - [9] C. Honerkamp and M. Sigrist, Prog. Theor. Phys. **100**, 53 (1998); M. Yamashiro, Y. Tanaka, and S. Kashiwaya, J. Phys. Soc. Jpn. **67**, 3364 (1998).
 - [10] M. Sigrist *et al.*, Physica C **317-318**, 134 (1999).
 - [11] Y. Yoshida *et al.*, J. Phys. Soc. Jpn. **68**, 3041 (1999); S. NishiZaki, Y. Maeno, and Z. Q. Mao, J. Phys. Soc. Jpn. **69**, 572 (2000).
 - [12] K. Ishida *et al.*, Phys. Rev. Lett. **84**, 5387 (2000).
 - [13] D. F. Agterberg, T. M. Rice, and M. Sigrist, Phys. Rev. Lett. **78**, 3374 (1997).
 - [14] K. Miyake and O. Narikiyo, Phys. Rev. Lett. **83**, 1423 (1999); Y. Hasegawa, K. Machida, and M. Ozaki, J. Phys. Soc. Jpn. **69**, 336 (2000).
 - [15] D. I. Khomskii and A. Freimuth, Phys. Rev. Lett. **75**, 1384 (1995).
 - [16] G. Blatter *et al.*, Phys. Rev. Lett. **77**, 566 (1996).
 - [17] N. Hayashi, M. Ichioka, and K. Machida, J. Phys. Soc. Jpn. **67**, 3368 (1998).
 - [18] J. Goryo, Phys. Rev. B **61**, 4222 (2000).
 - [19] N. Hayashi, private communication.
 - [20] M. Matsumoto and M. Sigrist, J. Phys. Soc. Jpn. **68**, 724 (1999).
 - [21] R. Heeb, Doctor thesis, ETH Zürich (2000).
 - [22] D. F. Agterberg, Phys. Rev. Lett. **80**, 5184 (1998); Phys. Rev. B **58**, 14484 (1998).
 - [23] R. Heeb and D. F. Agterberg, Phys. Rev. B **59** 7076 (1999).
 - [24] F. Gygi and M. Schlüter, Phys. Rev. B **43**, 7609 (1991).
 - [25] G. E. Volovik, Pis'ma Zh. Éksp. Teor. Fiz. **70**, 601 (1999) [JETP Lett. **70**, 609 (1999)].
 - [26] M. Matsumoto and M. Sigrist, Physica B **281&282**, 973 (2000).
 - [27] K. U. Neumann *et al.*, Eur. Phys. J. B **1**, 5 (1998).
 - [28] K. Kumagai, K. Nozaki, and Y. Matsuda, preprint, cond-mat/0012492.